On the evolution of salt lakes: Episodic convection beneath an evaporating salt lake

D. A. Nield,[1] C. T. Simmons,[2] A. V. Kuznetsov,[3] and J. D. Ward[2]

Received 9 May 2007; revised 6 September 2007; accepted 31 October 2007; published 28 February 2008.

[1] The transient evolution of salt lake brines and the accompanying underlying groundwater salinity distribution with depth is discussed. A convective-diffusive equation with a novel surface source term modeling the evaporative process is introduced, and an approximate analytical solution of this equation is obtained using a perturbation approach. A linear stability analysis of the resulting solution is carried out. For typical field-scale parameters, the model predicts that instability may initially occur within timescales on the order of weeks or decades and that a near-surface layer of salty fluid whose thickness is on the order of decimeters is responsible for the initial onset of convection. Furthermore, the analysis indicates that when convection starts, the decimeter layer mixes, and this results in the loss of the destabilizing force. In this period, the salty fluid diffuses downward. This results in a return to a hydrologic system, where the salt profile is then well mixed throughout, but now with a background concentration with a higher average salinity. The process can then repeat for an extensive but finite period as the surface layer and subsurface groundwater concentration eventually become hypersaline and where salt precipitation occurs. We have called this phenomenon episodic convection. Variable-density groundwater flow and solute transport modeling experiments of a field-based salt lake system confirm the existence of episodic convection and semiquantitatively validate the findings of the analytical approach.

Citation: Nield, D. A., C. T. Simmons, A. V. Kuznetsov, and J. D. Ward (2008), On the evolution of salt lakes: Episodic convection beneath an evaporating salt lake, *Water Resour. Res.*, *44*, W02439, doi:10.1029/2007WR006161.

1. Introduction

[2] Salt pans, playas, sabkhas, salinas, saline lakes, and salt flats are ubiquitous features in arid and semiarid areas of the earth [*Yechieli and Wood*, 2002]. They are similar in hydrologic terms, and as these authors correctly note, these systems vary only in the nature of their boundary conditions. The main requirement for the occurrence of such a saline system is that evaporation exceeds precipitation [*Yechieli and Wood*, 2002]. Authors such as *Yechieli and Wood* [2002], *Rosen* [1994], and *Tyler et al.* [2006] provide an excellent summary of research work relating to the origins of saline systems such as salt lakes, the hydrologic processes occurring in them, the role of groundwater in playas and the role of climate in driving hydrological processes. The reader is therefore referred to these earlier works for an exhaustive treatment on previous salt lake research and related studies.

[3] In the past several authors have described the process of brine reflux in shallow playa groundwater systems [*Duffy and Al-Hassan*, 1988; *Macumber*, 1991; *Wooding et al.*, 1997a, 1997b; *Simmons et al.*, 1999; *Fan et al.*, 1997] and the possibility that density-driven flow processes may result in complex groundwater hydrodynamics beneath a salt lake. Indeed, in such systems, there is the potential for unstable fluid motion to occur owing to the density stratification (i.e., salt lake brines of higher density overlying groundwater of lower density). Density-driven convection may lead to the circulation of brine throughout the entire aquifer. The density-driven convection process is an effective solute transport and mixing mechanism, moving salt more rapidly and over larger spatial scales when compared with diffusion alone. As noted by *Holzbecher* [2005], dense brines produced from surface evaporation can overturn and sink in the central portions of playas, setting up large-scale circulation cells in the deep underlying groundwater system. These convective cells resurface at the margins of the salt playas, where the dense brines mix with incoming fresh groundwater. Authors such as *Holzbecher* [2005], *Wooding et al.* [1997a, 1997b], *Wooding* [2007], *Simmons et al.* [1999], and *Duffy and Al-Hassan* [1988] have developed numerical models to simulate the density-driven flow processes beneath salt lake systems. An excellent summary of previous numerical modeling efforts is provided by *Holzbecher* [2005]. These modeling studies begin to elucidate the key density-driven flow processes that occur beneath a salt lake system. However, there are no really detailed numerical studies that model in precise terms the simultaneous hydrologic and salinity evolution of salt lake systems from genesis to maturity, i.e., over very long timescales of tens to hundreds of thousands of years. As noted by *Yechieli and*

[1]Department of Engineering Science, University of Auckland, Auckland, New Zealand.
[2]School of Chemistry, Physics and Earth Sciences, Flinders University, Adelaide, South Australia, Australia.
[3]Department of Mechanical and Aerospace Engineering, North Carolina State University, Raleigh, North Carolina, USA.

0043-1397/08/2007WR006161$09.00

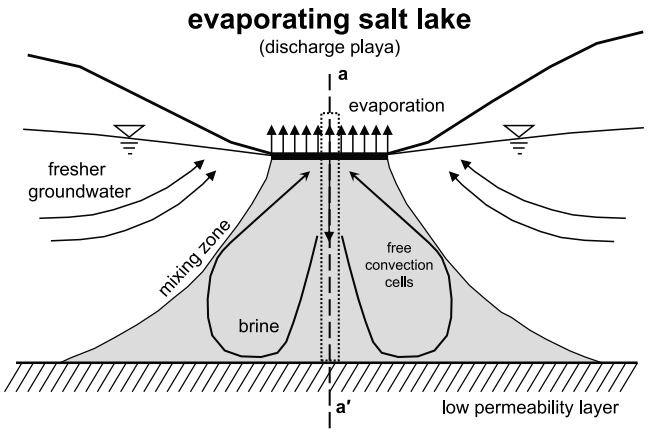

Figure 1. Conceptual model of a field-based discharge playa. No open water ponding exists, and evaporation occurs directly from the soil sediment. Groundwater discharges to the playa surface, and evapoconcentration accumulates salt in the near-surface soil profile of the playa. A concentration gradient (salty fluid over fresher groundwater) may establish, and density-driven free convection circulates the brine throughout the aquifer layer. Mathematical analyses performed in this paper occur along the line of symmetry a-a′ (the line representing purely vertical upward groundwater discharge), as indicated by the dashed box.

Wood [2002], while saline water bodies are widespread arid environments, they usually represent transient conditions. It is, therefore, frequently necessary to account for past hydrological conditions in hydrologic analyses. Elucidating evolutionary hydrodynamic and solute transport behavior over long historic timescales poses particular challenges in hydrologic analyses and remains largely unexplored and poorly understood. However, this exemplifies the need for a quantitative assessment of the evolutionary behavior of salt lake systems from both a theoretical viewpoint as well as in more practical terms by way of field-based experimentation. Indeed, a greater understanding of the evolutionary behavior from a hydraulic and theoretical viewpoint is expected to be important in directing future field-based analyses and investigations. This may also aid in the more accurate interpretation of salt and water balances, isotope signatures, and other related hydrologic, hydrochemical, hydrogeologic, and climatological data that are pertinent to salt lake studies.

[4] Some authors have attempted to quantify the nature of the density-driven flow process using the Rayleigh number (Ra), a dimensionless number that represents the ratio of buoyancy driven flow (that drives convective circulations) to diffusive/dispersive transport (that dissipates convective circulations). Previous literature (see *Nield and Bejan* [2006] for an exhaustive review) shows that the Rayleigh number is the critical controlling parameter for the onset of density-driven convection. Indeed authors including *Simmons et al.* [1999, 2002], *Wooding et al.* [1997a, 1997b], *Rogers and Dreiss* [1995], *Sanford and Wood* [2001], and *Holzbecher* [2005] have used Rayleigh stability criteria, in various forms, to characterize density-driven flow processes in these salt lake and saline hydrologic settings. Most often, the criterion used for the onset of free convection in porous media (and hence in these convective analyses of salt lake systems) is that the critical Rayleigh number is $4\pi^2$ [*Horton and Rogers*, 1945; *Lapwood*, 1948]. This stability criterion makes certain assumptions about the nature of the upper and lower boundary conditions of the infinite porous layer, namely impervious, "conducting" boundaries, and it is assumed that the basic density gradient is uniform. It is, however, not immediately clear whether this is the most appropriate stability criterion for a salt lake environment, particularly where there is an evaporating discharge boundary at the upper surface. This vertical flux is not accounted for in the boundary conditions that lead to the commonly used critical Rayleigh number noted above. An investigation of the appropriate stability criteria is therefore also critically required.

[5] In this study we attempt to explore the transient evolution of salt lake brines and the accompanying underlying groundwater salinity distribution with depth. We use a theoretical development based upon a stability analysis of the appropriate governing equations and then conduct numerical experiments using a variable-density groundwater flow model to validate those findings. The analysis presented here is motivated by questions that are particularly focused on transient salt lake evolutionary phenomena and the associated (transient) density-driven convective processes. These include, for example, the following.

[6] 1. How does a salt lake evolve from genesis to maturity over longer geologic timescales and what are the hydrologic processes that occur throughout its evolution? What are the mechanisms for salt accumulation and reflux beneath the salt lake and the underlying groundwater system? What are the associated spatial and temporal scales for these reflux and solute transport processes?

[7] 2. Are commonly used Rayleigh stability criteria (such as $Ra_c = 4\pi^2$) appropriate in the analysis of density-driven flow in a salt lake environment, especially noting the presence of an upward flux associated with evaporative discharge at the salt lake boundary? Are current Ra stability assessments used in previous literature too simple to be useful in the assessment of density-driven convective phenomena associated with brine reflux?

[8] 3. What are the states of stability and instability in the system throughout time? Is the system always unstable? How do the physical factors compete in these accumulation and reflux processes? For example, evaporative discharge leads to salt accumulation at the salt lake surface but diffusion/convection transport salt away from it. How do these processes manifest in time-dependent concentration profiles both at and beneath the evaporating salt lake, and throughout the vertical profile beneath the lake?

2. Conceptual Model

[9] Our salt lake conceptual model is based on a number of real world possibilities as outlined by *Yechieli and Wood* [2002] who have noted that physical processes among saline systems including salt lakes and sabkhas are often very similar but vary in their boundary conditions. We therefore choose one possible set of boundary conditions based upon an evaporating discharge playa. Consider a discharge playa (or salt lake) as shown in Figure 1. Since this is the first analysis of its kind, we start with the assumption that the groundwater system is both homogeneous

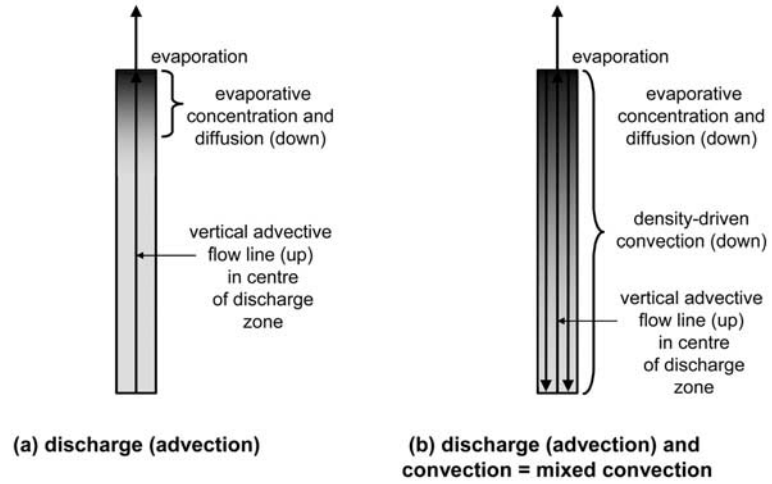

Figure 2. Two dominant groundwater flow and solute transport regimes that are likely to occur in nature. These are denoted as (a) the discharge regime (advection-only), where evapoconcentration and diffusion are dominant, and (b) the discharge (advection) and convection (and hence mixed convection) regime, where density-driven flow mixes salt vertically throughout the profile. Evapoconcentration and diffusion still occur in this second regime, but they are small compared with the free convective (density-driven) process.

and isotropic. Groundwater flow is directed toward the discharge feature where it evaporates. It is important to note that there is no surface ponding in this system. All salt accumulation occurs in the soil sediments immediately beneath the playa surface. In an idealized setting, the flow system may be considered symmetrical about the line a−a′. The line of symmetry is a groundwater divide. It is important because it represents a purely vertical and upward flow line along which to perform a one-dimensional (1-D) analysis as required by the analytical approach presented below. Assuming that no salt crust is yet developed on the surface of the playa, the surficial evaporation rate through the soil may be of the order of 100 mm/a [*Yechieli and Wood*, 2002] and is substantially lower than that of a ponded open water body. Flow continuity between the surface and porous medium requires that the vertical flow rate in the porous layer is therefore obtained by dividing this evaporation rate by the porosity of the sediment. Our analysis is purely 1-D and is taken by assuming flow continuity along the vertical flow line. Two dominant groundwater flow and solute transport regimes, as outlined in Figure 2, are likely to occur in nature. These are denoted as (1) the discharge regime (advection-only) and (2) the discharge (advection) and convection (and hence mixed convection) regime. In the first, groundwater discharge (advection) is dominant. Here, upward flow occurs toward the discharge playa and evaporation leads to the concentration of salts in the surface layer. A concentration gradient (saltier fluid at surface and fresher groundwater at depth) builds up progressively through evapoconcentration. This leads to diffusion of salts vertically downward into the profile. If evapoconcentration occurs at a rate that exceeds the diffusive losses, we expect that the concentration gradient will continue to increase. At some point in time, we might expect that the concentration gradient may exceed some critical concentration gradient required for the onset of density-driven convection. Indeed, one would expect that when some critical Rayleigh number is exceeded, convection will begin. In this second regime, density-driven convective circulation is able to move the saltier fluids from the shallower parts of the profile and mix them through the subsurface profile. The convective process is both rapid and effective at mixing salt over larger distances and shorter timescales when compared to diffusion alone [*Simmons et al.*, 2001]. To be precise, this regime is mixed convective since both free convection (driven purely by density differences) and forced convection (driven by advection) act to control the solute transport process. Our analysis examines how these regimes act to control the salinity evolution in the discharge playa system throughout time. It is important to note that the notion of "episodic convection" proposed in this paper is one that was first conceived by the authors through intuitive logic and reasoning and that this preceded the mathematical analyses presented here. As will be shown in this paper, the analytical solutions and numerical groundwater modeling lend strong weight to our hypothesis. In the very least they suggest that this process is theoretically conceivable in a salt lake setting.

3. Theory

[10] It is proposed that one can model the development of a salt lake as a result of evaporation from the surface by the following system of equations.

[11] It is assumed that the lake has initially a uniform distribution of salinity C_0. For $t \geq 0$, $0 \leq z < \infty$, the salinity is denoted by $C^*(z, t)$ and we let $C(z, t) = (C^*(z, t) - C_0)/C_0$.

[12] To begin with, for the determination of the basic salinity profile, we suppose that the lake is of infinite depth. Later on, when we consider the stability problem, we will consider a layer of the finite depth and we will lop off the bottom of the basic salinity profile that we have previously obtained.

[13] Here the z-axis is taken vertically downward with origin at the surface. It is assumed that C satisfies the following system:

$$\frac{\partial C}{\partial t^*} - U\frac{\partial C}{\partial z^*} = \kappa\frac{\partial^2 C}{\partial z^{*2}} + \sigma(t^*)\delta^*(z^* - 0^{*+}), \tag{1}$$

$$C = 0 \text{ at } t^* = 0, \tag{2}$$

$$\frac{\partial C}{\partial z^*} = 0 \text{ at } z^* = 0, \tag{3}$$

$$C \to 0 \text{ as } z^* \to \infty. \tag{4}$$

The asterisks denote dimensional quantities. It will be noted that the origin for the z^*-coordinate has been chosen to be just above the water surface, so that the evaporation effects are incorporated in the differential equation rather than in the boundary condition.

[14] Here U represents a constant upward flow (so that the velocity vector is $(0, 0, -U)$), κ is a constant diffusivity, $\sigma^*(t^*)$ represents the magnitude of a surface source, $\delta^*(z^*)$ is the Dirac delta function, and 0^{*+} is a very small positive constant. We introduce what we call the evaporation-diffusive length scale $L_{ed} = \kappa/U$ and the evaporation-diffusive timescale $T_{ed} = \kappa/U^2$. We introduce dimensionless variables z and t and a new source coefficient σ defined by

$$z = (U/\kappa)z^*, \quad t = \left(U^2/\kappa\right)T^*, \quad \sigma = \sigma^*/U \tag{5}$$

so that equations (1)–(4) become

$$\frac{\partial C}{\partial t} - \frac{\partial C}{\partial z} = \frac{\partial^2 C}{\partial z^2} + \sigma(t)\delta(z - 0^+), \tag{6}$$

$$C = 0 \text{ at } t = 0, \tag{7}$$

$$\frac{\partial C}{\partial z} = 0 \text{ at } z = 0, \tag{8}$$

$$C \to 0 \text{ as } z \to \infty. \tag{9}$$

The overall conservation of salt mass requires that

$$\int_0^\infty \left(-\frac{\partial C}{\partial z}\right)dz = \int_0^\infty \sigma(t)\delta(z - 0^+)dz \tag{10}$$

so that

$$\sigma(t) = C(0, t). \tag{11}$$

[15] It appears that this set of equations has no exact analytical solution. The presence in equation (6) of the convective term, containing a first spatial derivative, in combination with the boundary condition given by equation (8), thwarts an analytical attack. It is possible to eliminate the convective term from the differential equation using a coordinate transformation but this has the effect of replacing the Neumann (second kind) boundary condition by one of the Robin (third kind) type, and so there is no net analytical advance. In physical terms the Robin boundary condition corresponds to a leakage of species mass across the boundary (compare the Newtonian thermal boundary condition). However, an approximate analytical solution, useful for a certain range of parameters and variables, can be obtained using a perturbation procedure as follows.

[16] We anticipate that for small values of the time t the variable C will differ significantly from zero only in a shallow layer near the surface. In this circumstance the diffusive term involving $\partial^2 C/\partial z^2$ will dominate over the convective term involving $\partial C/\partial z$. Hence as a first approximation, we solve equations (6)–(9) for C without the convective term, obtaining a solution that we denote by $C_1(z, t)$. (Later, as a second approximation, we will repeat the process with $\partial C/\partial z$ approximated by $\partial C_1/\partial z$). Hence we write

$$\frac{\partial C_1}{\partial t} = \frac{\partial^2 C_1}{\partial z^2} + \sigma(t)\delta(z - 0^+), \tag{12}$$

$$C_1 = 0 \text{ at } t = 0, \tag{13}$$

$$\frac{\partial C_1}{\partial z} = 0 \text{ at } z = 0, \tag{14}$$

$$C_1 \to 0 \text{ as } z \to \infty. \tag{15}$$

[17] We introduce the Fourier cosine transform

$$F_c\{C_1(z,t)\} = \bar{C}(s_1, t) = \int_0^\infty C_1(z,t)\cos(s_1 z)dz. \tag{16}$$

Using integration by parts and equations (14) and (15), one obtains

$$F_c\left\{\partial^2 C_1(z,t)/\partial z^2\right\} = -s_1^2\bar{C}(s_1, t). \tag{17}$$

Then, taking the transform of equation (12), one has

$$\frac{d\bar{C}_1}{dt} + s_1^2\bar{C}_1 = \sigma(t). \tag{18}$$

Further, the transform of equation (13) gives

$$\bar{C}_1 = 0 \text{ at } t = 0. \tag{19}$$

The solution of equation (18) subject to equation (19) is

$$\bar{C}_1(s_1, t) = \int_0^t \sigma(\tau_1)e^{-s_1^2(t-\tau_1)}d\tau_1. \tag{20}$$

Finally, $C_1(z, t)$ is obtained using the inversion formula

$$C_1(z,t) = \frac{2}{\pi}\int_0^\infty \bar{C}_1(s_1,t)\cos(s_1 z)ds_1. \tag{21}$$

Hence we conclude that

$$C_1(z,t) = \frac{2}{\pi}\int_0^\infty \left(\int_0^t \sigma(\tau_1)e^{-s_1^2(t-\tau_1)}d\tau_1\right)\cos(s_1 z)ds_1. \tag{22}$$

Differentiating with respect to z under the integral sign, we get

$$\frac{\partial C_1(z,t)}{\partial z} = -\frac{2}{\pi}\int_0^\infty \left(\int_0^t \sigma(\tau_1)e^{-s_1^2(t-\tau_1)}d\tau_1\right)s_1\sin(s_1 z)ds_1. \tag{23}$$

At the next stage we solve

$$\frac{\partial C_2}{\partial t} = \frac{\partial^2 C_2}{\partial z^2} + \sigma(t)\delta(z-0^+) + \frac{\partial C_1(z,t)}{\partial z}, \tag{24}$$

$$C_2 = 0 \text{ at } t = 0, \tag{25}$$

$$\frac{\partial C_2}{\partial z} = 0 \text{ at } z = 0, \tag{26}$$

$$C_2 \to 0 \text{ as } z \to \infty. \tag{27}$$

Combining (23) and (24), we have

$$\frac{\partial C_2}{\partial t} = \frac{\partial^2 C_2}{\partial z^2} + \sigma(t)\delta(z-0^+) - \frac{2}{\pi}\int_0^\infty \left(\int_0^t \sigma(\tau_1)e^{-s_1^2(t-\tau_1)}d\tau_1\right)s_1\sin(s_1 z)ds_1. \tag{28}$$

We now proceed as before. We define

$$F_c\{C_2(z,t)\} = \bar{C}_2(s_2,t) = \int_0^\infty C_2(z,t)\cos(s_2 z)dz. \tag{29}$$

We find that

$$\bar{C}_2(s_2,t) = \int_0^t \left[\sigma(\tau_2) - \frac{2}{\pi}\int_0^\infty \left(\int_0^\infty \left(\int_0^{\tau_2}\sigma(\tau_1)e^{-s_1^2(\tau_2-\tau_1)}d\tau_1\right)\cdot s_1\sin(s_1\zeta_1)ds_1\right)\cos(s_2\zeta_1)d\zeta_1\right]e^{-s_2^2(t-\tau_2)}d\tau_2, \tag{30}$$

and so

$$C_2(z,t) = \frac{2}{\pi}\int_0^\infty \bar{C}_2(s_2,t)\cos s_2 z ds_1 = \frac{2}{\pi}\int_0^\infty \left\{\int_0^t \left[\sigma(\tau_2) - \frac{2}{\pi}\int_0^\infty \cdot\left(\int_0^\infty \left(\int_0^{\tau_2}\sigma(\tau_1)e^{-s_1^2(\tau_2-\tau_1)}d\tau_1\right)s_1\sin(s_1\zeta_1)ds_1\right)\cdot\cos(s_2\zeta_1)d\zeta_1\right]e^{-s_2^2(t-\tau_2)}d\tau_2\right\}\cos(s_2 z)ds_2. \tag{31}$$

Similarly, in principle, one can find $C_3(z, t)$ from $C_2(z, t)$, etc.

[18] We now assume that $\sigma(t)$ is a slowly varying function of t, and we can approximate it by its mean over a range of t from 0 to T, say,

$$\sigma_T = \frac{1}{T}\int_0^T \sigma(t)dt, \tag{32}$$

to get a rough approximation for $C_1(z, t)$. One finds that approximately

$$C_1(z,t) = \frac{2\sigma_T}{\pi}\int_0^\infty \left(1-e^{-s^2 t}\right)s^{-2}\cos(sz)ds = \sigma_T\left\{\sqrt{\frac{4t}{\pi}}e^{-z^2/4t} - z\ \mathrm{erfc}\left(\frac{z}{\sqrt{4t}}\right)\right\} = 2\sigma_T\sqrt{\frac{t}{\pi}}\left\{e^{-\xi^2} - \sqrt{\pi}\xi\mathrm{erfc}(\xi)\right\}, \tag{33}$$

where $\xi = z/\sqrt{4t}$.

[19] This is a self-similar solution. Figure 3 is a plot of equation (33) for the case $\sigma_T = 1$ for two cases (1) $z = 0$ (i.e., at the discharge playa surface) and (2) as a function of depth z below the surface. We include this as an illustration of the qualitative aspects of the solution. Importantly, it is clear that surface salinity increases with time but its mathematical form is slightly complicated as suggested by equation (33). The variation in salinity with time is greatest at the lake surface and decreases with increasing depth.

[20] The function

$$F(\xi) = e^{-\xi^2} - \sqrt{\pi}\xi\mathrm{erfc}(\xi) \tag{34}$$

decays from 1 to 0 as ξ increases, quite rapidly. In fact a graph shows that this function is practically indistinguishable from zero when $\xi > 2$. For example, $F(2) = 0.00173$.

[21] From equation (33) one finds that

$$C_1(0,t) = 2\sigma_T\sqrt{\frac{t}{\pi}}. \tag{35}$$

Employing this in equation (11) and averaging over the time interval $[0, T]$ gives

$$\sigma_T = \frac{4U\sigma_T}{3}\sqrt{\frac{T}{\pi}}. \tag{36}$$

One has consistency if one chooses T to have the value

$$T = \frac{9\pi}{16}. \tag{37}$$

Our rationale for the above procedure is the following. In order for the Fourier transform technique to be applicable we must assume that the magnitude of source term be independent of time. In other words, we need to "freeze" the value of $\sigma(t)$ at some constant value, and we have taken the expression in equation (32) as our best guess for this value. We propose the label "quasi-similarity solution" for the solution (given by equation (33)) obtained in this way.

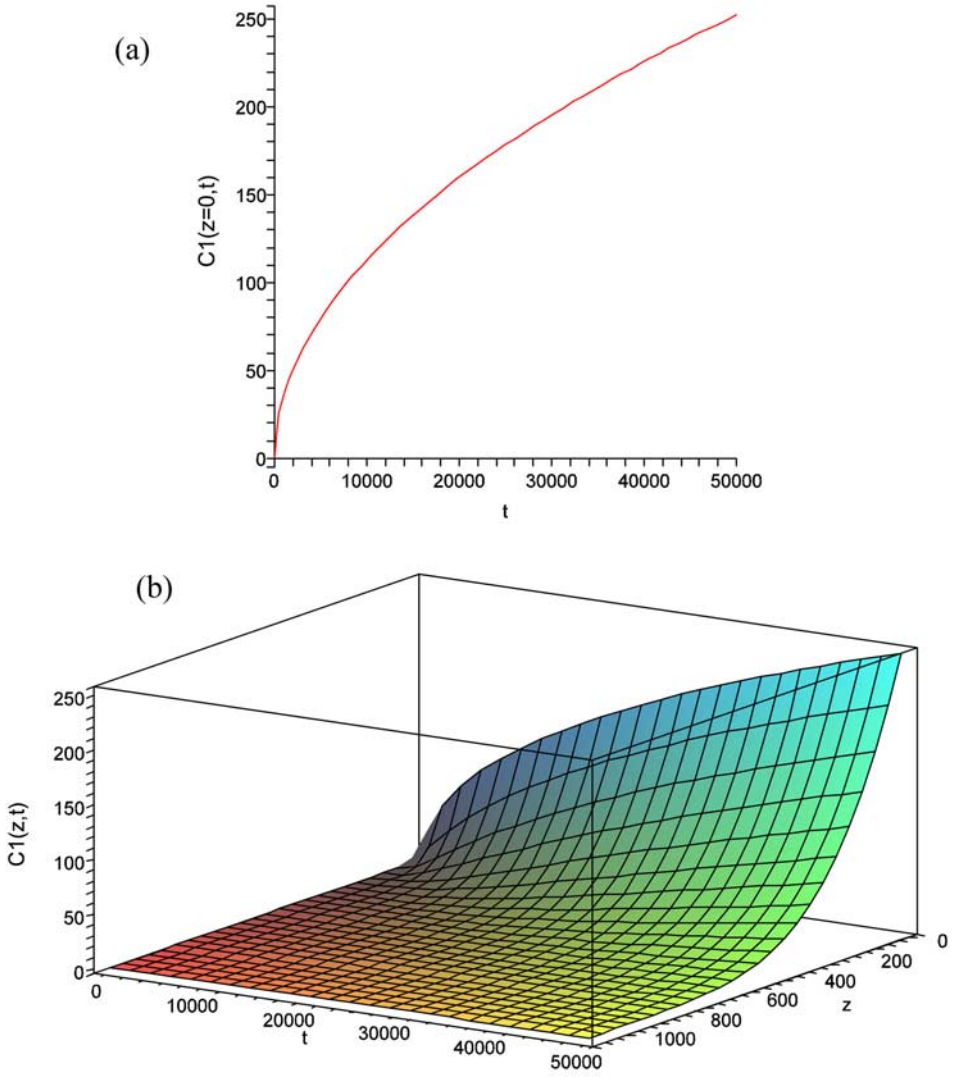

Figure 3. Plot of $C_1(z, t)$ in equation (33) for the case $\sigma_T = 1$ and for (a) $z = 0$ (i.e., at the discharge playa surface) and (b) as a function of depth z below the surface. Qualitative aspects of the solution are demonstrated, and increasing salinity with time is observed. Variation in concentration through time is largest at the surface and decreases with increasing depth.

[22] The calculation of C_2 requires the numerical evaluation of the inverse transform integral, the integral with respect to s_2, which is truncated at some value N. The effect of this is that large wave numbers are neglected and so some of the fine structure of the salinity profile is lost. We found that $N < 10$ led to loss of accuracy and that $N = 100$ led to nonsense because of accumulated round-off error, so we used the value $N = 40$ in most of our calculations of C_2.

[23] For the case $\sigma(t) = 1$, we have plotted C_1 and C_2 versus z for various values of t. We found that there are discrepancies for small values of t (e.g., C going negative before it becomes negligibly small) that are not surprising since when t tends to zero the similarity variable ξ tends to infinity. There are also major discrepancies when $t > 3$. This is not unexpected. The surface boundary layer can be expected to thicken as a result of diffusion as t increases, so that our assumption that $\partial C/\partial z$ is small compared with $\partial^2 C/\partial z^2$ is no longer valid. However, it appears that for $0.1 < t < 2$, C_2 behaves sensibly and is close to C_1. That means that there is a range of t for which the analytical solution equation (33) is a reasonable approximation. One can then use this for a qualitative investigation of stability.

[24] Without an open water body at the surface of the discharge playa, we may assume that the evaporation rate from the soil surface is on the order of $E = 100$ mm/a (to an order of magnitude estimate). Assuming a porosity of 0.3 consistent with a sandy material, the flow rate through the sandy layer is $U = 0.33$ m/a. If one assumes $\kappa = 0.03$ m^2/a then the relevant length scale is 0.1 m and the timescale is 0.3 years. These values are all consistent with reasonable estimates based upon realistic field observations.

[25] The above analysis is independent of the momentum equation, and hence independent of whether one has a porous medium or a fluid clear of solid material. In the remainder of the paper we consider a porous medium, and

we use the notation of *Nield and Bejan* [2006]. The Rayleigh-Darcy number Ra_D is defined as

$$\mathrm{Ra}_D = \frac{g\beta_C K H \Delta C}{\nu D_m}. \tag{38}$$

Here g is the gravitational acceleration, K is the permeability, H is the layer depth, ν is the kinematic viscosity of the fluid, and D_m is the effective diffusivity in the porous medium (the porosity times the diffusivity in the fluid), while ΔC is the concentration difference across the layer and $\beta_C \Delta C$ is the fractional change in density across the layer. The diffusivity κ employed above can now be identified with D_m.

[26] We consider that part of the profile in which there is a significant variation of concentration. We note that equation (35) gives the surface concentration, and the concentration drops down to almost zero when $\xi = 2$, where $\xi = z/\sqrt{4t}$. Thus we can consider a layer for which the concentration difference is equal to the surface concentration and the layer depth is $z_e = 4t^{1/2}$.

[27] We suppose that the layer has an impervious top at constant concentration and a free bottom at constant concentration. The standard linear stability theory [see, e.g., *Nield*, 1975], leads to the following boundary value problem:

$$\left(D^2 - a^2\right) W = -\mathrm{Ra}_D a^2 \Gamma, \tag{39}$$

$$\left(D^2 - a^2\right) \Gamma = -f(\zeta) W, \tag{40}$$

$$W = \Gamma = 0 \text{ at } \zeta = 0, \tag{41}$$

$$DW = \Gamma = 0 \text{ at } \zeta = 1. \tag{42}$$

Here $W(\zeta)$ and $\Gamma(\zeta)$ are respectively velocity and concentration amplitude functions, D denotes the operator $d/d\zeta$, a is a horizontal wave number, and $f(\zeta)$ denotes the salinity gradient normalized by the requirement that $\langle f(\zeta) \rangle = 1$, where the angle brackets denote an integral with respect to ζ from 0 to 1. The system consisting of equations (39)–(41) can be solved approximately using a Galerkin method. Suitable trial functions that satisfy the boundary conditions are

$$W = 2\zeta - \zeta^2, \quad \Gamma = \zeta - \zeta^2, \tag{43}$$

and the method yields

$$\mathrm{Ra}_D = \frac{\langle (DW)^2 + a^2 W^2 \rangle \langle (D\Gamma)^2 + a^2 \Gamma^2 \rangle}{a^2 \langle W\Gamma \rangle \langle W\Gamma f(\zeta) \rangle}. \tag{44}$$

For example, when $f(\zeta) \equiv 1$, this formula gives

$$\mathrm{Ra}_D = \frac{32(5 + a^2)(10 + a^2)}{49 a^2}. \tag{45}$$

This is minimized when $a = \sqrt{5}$, and the minimum value of Ra_D is 29.4. This exceeds by about 8.5% the exact value 27.1. This value was originally obtained by *Nield* [1968] and is cited by *Nield and Bejan* [2006, Table 6.1].

[28] To apply formula (44) to the present problem we make the following connections. We suppose that the bottom boundary corresponds to $\xi = \alpha$, where α has a value near 2, and take $\zeta = \xi/\alpha$. Using equations (33) and (34) and the fact that $dF/d\xi = -\sqrt{\pi}\,\mathrm{erfc}(\xi)$, we then have

$$-\frac{dC_1}{d\zeta} = -\frac{dC_1}{dz}\frac{dz}{d\xi}\frac{d\xi}{d\zeta} = 2\alpha\sigma_T \sqrt{\frac{t}{\pi}}\,\mathrm{erfc}(\alpha\zeta), \tag{46}$$

and this requires that we take

$$f(\zeta) = \frac{\mathrm{erfc}(\alpha\zeta)}{\langle \mathrm{erfc}(\alpha\zeta) \rangle}. \tag{47}$$

Thus the net effect of the nonuniformity of the salinity gradient is to multiply the critical value of the Rayleigh number by the factor η where

$$\eta(\alpha) = \frac{\langle W\Gamma \rangle \langle \mathrm{erfc}(\alpha\zeta) \rangle}{\langle W\Gamma\,\mathrm{erfc}(\alpha\zeta) \rangle}, \tag{48}$$

where W and Γ are given by equation (43).

[29] At the same time, the bottom-to-top concentration difference is reduced by a factor $\varepsilon(\alpha) = 1 - F(\alpha)$ because of the selection of the lower boundary at $\xi = \alpha$. Taking this into account, the value of the critical number should also be divided by $\varepsilon(\alpha)$. Hence we calculated the function $\lambda(\alpha) = \eta(\alpha)/\varepsilon(\alpha)$, and we found that it has a minimum value of 1.29 at $\alpha = 1$ and increases to 1.74 at $\alpha = 2$.

[30] To counteract this increase in the value of the critical number one should note that the boundary condition equation (42) is more restrictive than is physically warranted, so that by using this boundary condition we overestimate Ra_{Dc}. Thus taking all these things into account, we use the estimate $\mathrm{Ra}_{Dc} = 30$.

4. Application of Theory to a Salt Lake System

[31] As an illustrative example, let us consider the following reference case, denoted by the subscript r:

$$g_r = 10 \text{ ms}^{-2},\ K_r = 10^{-12} \text{ m}^2,\ \nu_r = 10^{-6} \text{ m}^2 \text{ s}^{-1},$$
$$D_{mr} = 10^{-9} \text{ m}^2 \text{ s}^{-1},\ \beta_{Cr}\Delta C_r = 0.03,\ H_r = 0.1 \text{ m}.$$

These lead to $\mathrm{Ra}_{Dr} = 30$, which is equal to our estimate of the critical value.

[32] Relative to all of this we now have a layer depth (units 0.1 m) varying with time (units 0.3 years) as

$$z_e = 4t^{1/2} \tag{49}$$

and a concentration difference varying with time as

$$C(0,t) = 2\sigma_T \left(\frac{t}{\pi}\right)^{1/2}, \tag{50}$$

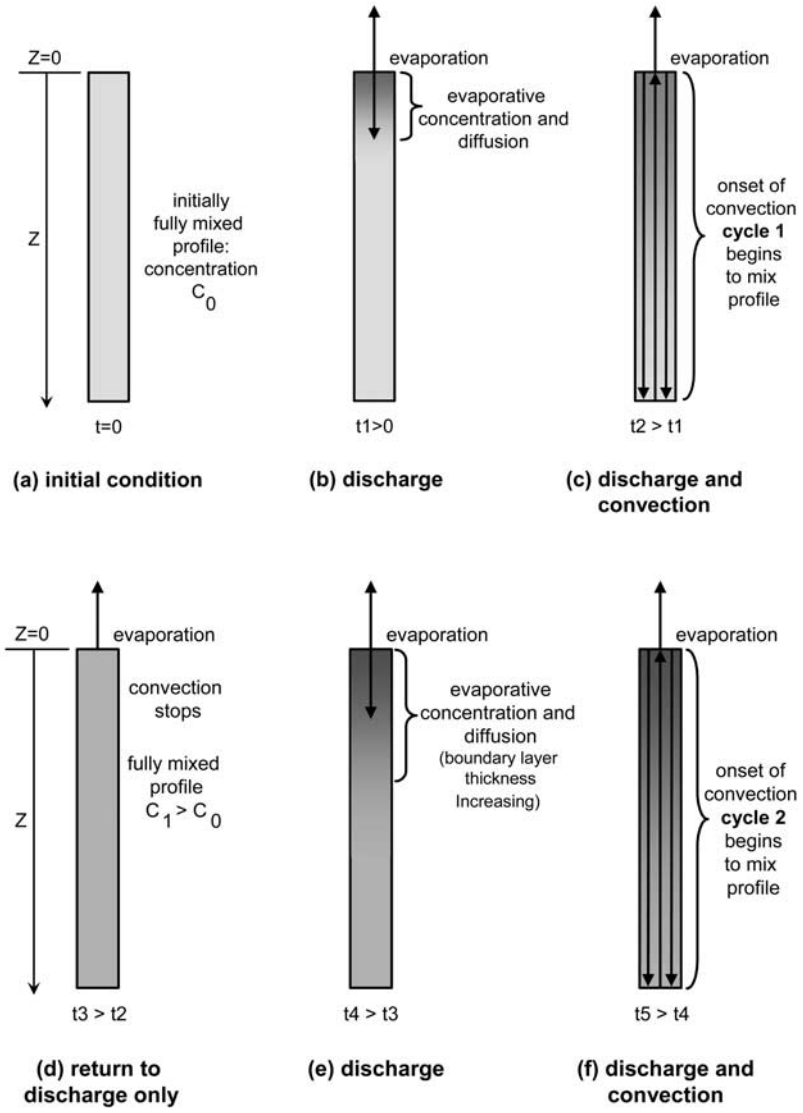

Figure 4. A conceptual schematic illustrating the various solute transport processes that occur through two cycles of the episodic convection process. The two major transport regimes shown in Figure 2 are seen to occur at different times and are interleaved through episodic repetition, i.e., discharge and evaporative concentration in the advection-only regime, and then discharge (advection) as well as density-driven free convection in the mixed convection regime. Increasing time snapshots t_i from the initial condition t_0 are shown.

so we have

$$\mathrm{Ra}_D/\mathrm{Ra}_{Dr} = \frac{8\sigma_T t}{\pi^{1/2}}. \tag{51}$$

[33] For the onset of convection, with the permeability measured in Darcys and a 3% initial solution, we thus estimate that $z_e C(0, t) = 1$ or $t = t_{\mathrm{crit}}$ where

$$t_{crit} = \pi^{1/2}/8\sigma_T = 0.22/\sigma_T \tag{52}$$

in terms of a timescale of 0.3 years.

[34] Thus for a porous medium with a permeability of 1 Darcy, one would expect instability after a couple of weeks. (We assume that σ_T is of order unity. Thus t_{crit} is of order 0.2, giving a dimensional time of order 0.06 years). For a medium with a permeability of 10^{-3} Darcy the time to instability would be a thousand times greater, that is a few decades.

[35] When convection starts, that decimeter layer gets mixed up and there is then no destabilizing agency, and the salty fluid diffuses downward. Then the net effect is that we are back to square one but with a higher average salinity in the system. The process can then repeat for an extensive period. We call this phenomenon episodic convection. A conceptual diagram given in Figure 4 illustrates the various solute transport processes that occur through two cycles of this episodic convection process. The two major transport regimes outlined earlier are seen to occur at different times and are interleaved, i.e., discharge and evaporative concentration in the advection-only regime, and then discharge (advection) as well as density-driven free convection in the

mixed convection regime. Increasing time snapshots t_i from the initial condition t_0 are shown. The process is expected to repeat for an extensive but finite period as the surface layer and subsurface groundwater concentration eventually become hypersaline. The upper time limit is dictated by the time it takes for precipitation of salts to occur. When precipitation occurs, the salt is effectively removed from the solute transport process. As the system gets increasingly more saline through progressive cycles and approaches halite precipitation levels, it is expected that the concentration gradients will become smaller. Intuitively, one may expect that the system would be most dynamic at early times (where maximum density contrasts can be established) but become increasingly lethargic at later times (where density contrasts progressively dissipate through repeated convection cycles that lead to mixing of the profile to new and higher concentrations, as well as the upper limit on salt concentrations that may be achieved as imposed by natural salt solubility limits).

[36] One can now estimate the timescale for mixing as follows. Near the onset of convection (for slightly supercritical Rayleigh number) the characteristic velocity scale is $U_{\mathrm{conv}} \sim (D_m/H)(\mathrm{Ra}_D - \mathrm{Ra}_{Dc})$ and hence the characteristic time for the convection circulation is $T_{\mathrm{conv}} = H/U_{\mathrm{conv}}$ or $(H^2/D_m)\ (\mathrm{Ra}_D - \mathrm{Ra}_{Dc})^{-1}$. If we take $H = O(L_{ed})$ and identify κ and D_m then $H^2/D_m = O(T_{ed})$. Hence $t_{\mathrm{conv}} = T_{\mathrm{conv}}/T_{ed} = O((\mathrm{Ra}_D - \mathrm{Ra}_{Dc})^{-1})$. We have a situation where Ra_D is increasing linearly with time. It is reasonable to expect that it will increase beyond the critical value for a time t_{conv} before mixing takes place and so the mean value of $\mathrm{Ra}_D - \mathrm{Ra}_{Dc}$ during this interval will be $\mathrm{Ra}_{Dc}t_{\mathrm{conv}}/2t_{\mathrm{crit}}$. The requirement for consistency is that

$$t_{\mathrm{conv}} = O\left(\left[\frac{2t_{\mathrm{crit}}}{\mathrm{Ra}_{Dc}}\right]^{1/2}\right) = O\left(\left[\frac{t_{\mathrm{crit}}}{15}\right]^{1/2}\right). \tag{53}$$

[37] One could expect to be in the domain of monotonic convection (hot salty fluid on top) so that one can add thermal and solutal Rayleigh numbers. The thermal Rayleigh number will be negative, and hence the onset of instability will be delayed by the thermal effect.

[38] A gradually increasing average density will result in a proportionately increasing destabilizing density gradient in the surface layer, and hence the value of t_{crit} is expected to decrease with time as the salt layer evolves.

5. Numerical Experiments

[39] Field verification of the theory described above is very difficult, if not impossible, owing to the potentially very long timescales of convection, and also the impracticality of observing concentration distributions at the scale and spatial resolution required to verify that episodic convection is occurring. One option that exists to verify the analytical theory is to perform a variable-density numerical simulation of the evapoconcentration process below a discharging salt lake. We perform some numerical experimentation here to lend support to the newly proposed analytical theory. Importantly, within a numerical framework many of the simplifying assumptions made in the development of the analytical solution are not required. The numerical modeling presented here is intended to be demonstrative rather than exhaustive since there are clearly a large number of boundary conditions in a variety of saline hydrologic systems [*Yechieli and Wood*, 2002]. Here, we wish to capture the essential processes of evaporative discharge and salt accumulation which are common to most, if not all, saline systems. Some key questions arise: do we observe episodic convection beneath a discharging salt lake in the numerical modeling framework? What are the spatial and temporal scales of the groundwater flow and solute transport processes observed? What does episodic convection look like in a framework that is 2-D or 3-D (removing the dimensionality restriction required of the 1-D analytical theory)?

[40] Numerical modeling was performed using FEFLOW version 5.2 [*Diersch*, 2005]. FEFLOW is a numerical finite element system that allows various 2-D projections as well as 3-D flow and transport processes in porous media. The code has been successfully benchmarked for a number of variable-density flow examples, such as the Elder, Henry, Salt Dome and Salt Pool problems [*Diersch and Kolditz*, 2002; *Diersch*, 2005]. The fundamental mathematical basis of FEFLOW [*Diersch*, 2005] is formed by the physical principles of mass conservation of a phase, contaminant mass conservation of a phase, and momentum conservation of a phase. The reader is referred to *Diersch* [2005] for further information relating to the FEFLOW variable-density groundwater flow model.

5.1. Conceptual Model

[41] For the purposes of a preliminary numerical demonstration, a 2-D vertical projection was chosen to model a vertical section highlighted in Figure 1, i.e., a region directly below the discharge playa. We focus the modeling framework on processes occurring directly beneath the discharge playa where groundwater flow is subvertical to vertical. A transient, density-dependent groundwater flow and solute transport regime was constructed. Figure 5 illustrates the basic concept and boundary conditions. The model has an initial concentration of about seawater (35,000 mg/L) throughout, which may be representative of a near-coastal sabkha system or discharge playa. Saltwater flows into the model at the bottom while evaporation occurs at the top surface. The side boundary conditions are assumed to be no flow in this analysis. The volumetric inflow rate at the bottom boundary was constant at 0.4 m^3/a and this corresponds to an evaporation rate of 10 mm/a at the top boundary (if we assume continuity along the vertical flow line in near-steady conditions). An evaporation rate in the range 10–100 mm/a is reasonable for a system where there is no surface water, where salinity is high and approaching precipitation levels. Evaporation is expected to be lowest when a salt precipitate crust has formed.

[42] Inflow of fluid was simulated via a fluid source term along the bottom row of elements, with a Neumann (flux) type mass boundary condition (constant rate of solute influx, commensurate with the inflow of fluid to simulate inflow of saltwater). Outflow was simulated via a sink term (equal magnitude to the inflow source term). Saltwater therefore enters the model at the bottom boundary condition but only water leaves the model at the upper boundary, therefore allowing salt accumulation to occur through

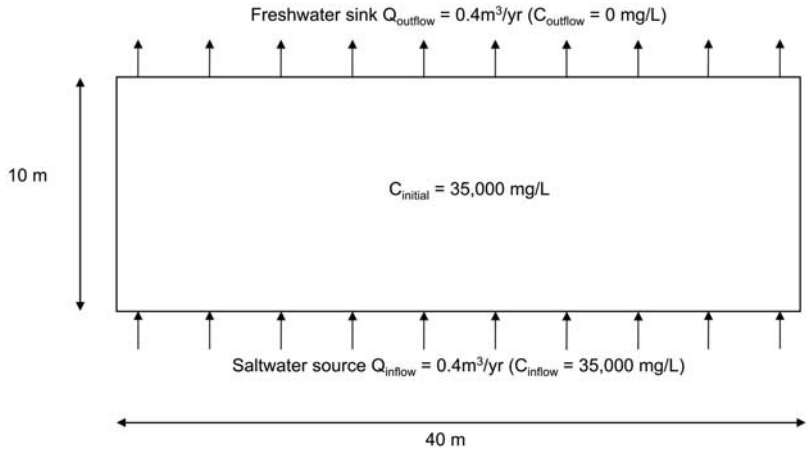

Figure 5. Conceptual model for FEFLOW simulation of groundwater flow and solute transport in an aquifer directly beneath a discharging playa. The bottom boundary condition is a salty fluid source, and evaporation (i.e., a fluid sink removing freshwater only) occurs at the top boundary condition at a rate of E = 10 mm/a. Side vertical boundaries are no flow boundaries.

evapoconcentration. A complete list of modeling parameters is shown in Table 1.

5.2. Spatial and Temporal Discretization

[43] The 2-D model domain was chosen as 40 meters long and 10 m high, and was discretized into 27,200 rectangular elements. While this choice is reasonably arbitrary, it should be noted that in steady state convective systems square cells (cell width = layer height) are expected to form. It is also known from previous Rayleigh stability criterion work that the critical Rayleigh numbers are approximately geometry independent where the box length is greater than about four times its height [*Caltagirone*, 1982; *Weatherill et al.*, 2004]. The chosen model domain therefore allows an integral number of larger steady cells to form at later times and has a sufficient aspect ratio to ensure that numerical results are not geometrically dependent. Numerical elements had a constant width of 0.1 m but varied in height. From the top of the model, the top 10 rows were of height 0.1 m (square elements), followed by 14 rows of height 0.14286 m, followed by 20 rows of height 0.2 m, 14 rows of height 0.14286 m, and finally 10 rows of height 0.1 m. This provided a symmetrical grid (symmetric about the horizontal, halfway up the grid) and a high level of discretization around the top and bottom boundaries to capture the potentially high density gradients. Some sensitivity analyses to spatial discretization were performed to ensure model results were relatively grid independent and confirmed that the above spatial discretization was satisfactory.

[44] It is important to estimate the evolution timescales in salt lake brine formation as this dictates numerical simulation time requirements. *Yechieli and Wood* [2002] present a simple analysis for estimating the evolution time for playa brine formation. Using the parameters employed in our numerical model, it is estimated (using equation (11) in *Yechieli and Wood*'s [2002] paper) that the time taken for our system to reach halite precipitation levels (~300,000 ppm) is about 2,500 years. As will be seen below, the episodic

Table 1. FEFLOW Numerical Modeling Parameters

Parameter	Symbol	Value	Unit
	Model		
Model length	x	40	m
Model width	z	10	m
Element width	Δx	0.1	m
Element height	Δz	varied, 0.1–0.2	m
	Aquifer Properties		
Hydraulic conductivity	K	8.64	m d^{-1}
Effective porosity	ε	0.3	–
Longitudinal dispersivity	β_L	0.2	m
Transverse dispersivity	β_T	= 0.1β_L	m
Molecular diffusivity	D_f	10^{-9}	m^2 s^{-1}
	Flow and Solute Conditions		
Volumetric inflow rate	Q_{inflow}	0.4	m^3/a
Volumetric outflow rate (evaporative discharge)	Q_{outflow}	0.4 (compare E = 10 mm/a)	m^3/a
Inflowing water concentration	C_{inflow}	35,000	mg L^{-1}
Outflowing water concentration	C_{outflow}	0	mg L^{-1}
Initial water concentration	C_{initial}	35,000	mg L^{-1}
Coefficient of density coupling with concentration	$\Delta\rho/\Delta C$	700	kg m^{-3}

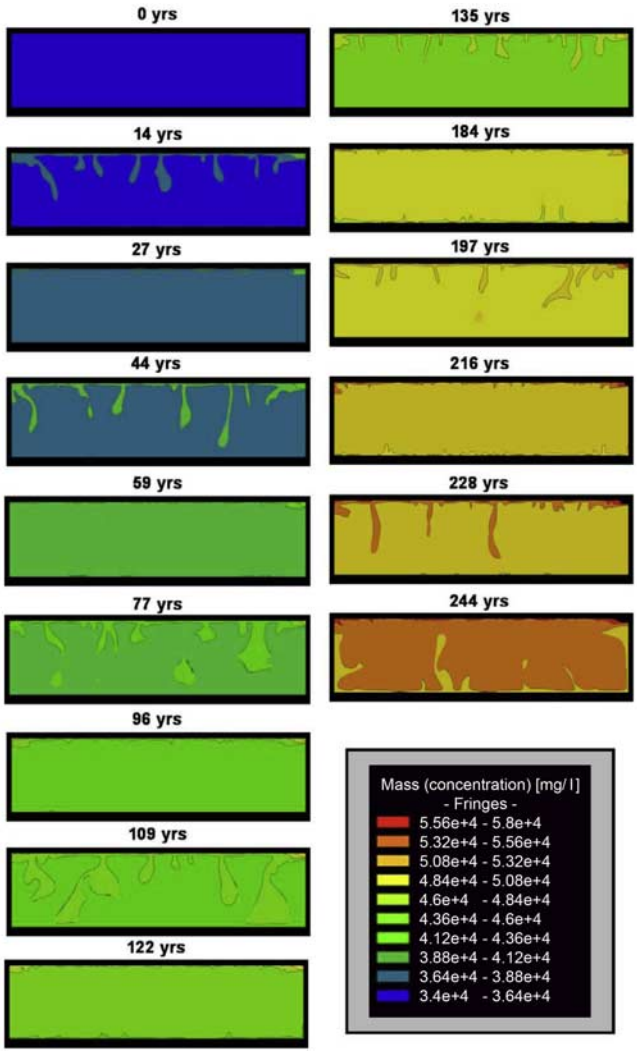

Figure 6. Numerical results for concentration distribution at various times, illustrating the episodic convection process. Shown are "birth" and "death" stages of fingering at the beginning and end of each episodic convection cycle. In this numerical example, the time between sequential new birth episodes as well as their intermediate persistence timescales occurs on decadal timescales.

convection process occurs on decadal timescales and therefore we may expect that up to several hundred episodic convection cycles may occur throughout the evolution of the salt lake from genesis to maturity. The computational power required to run this model was both extensive and extremely restrictive on even the fastest quad-processor PC available to us. As such, we have constrained our demonstrative verification activity to the primary requirement of observing several cycles of episodic convection only. We have necessarily relaxed the requirement of simulating the salt lake through to mature brine formation (halite precipitation levels). On the basis of this brine evolution analysis and the inherent computational complexity involved, we employ the following temporal parameters in our numerical simulation. The initial time step was 0.001 days, with time steps automatically increased (and decreased) throughout the simulation by FEFLOW. A maximum time step of 10 days was set. In FEFLOW, the automatic time step increment is regulated by error checking (based on a maximum error norm of 0.0001) and time steps are decreased when appropriate to reduce numerical instability based upon Courant type stability criteria. The total time of the simulation was 240 years (which was shown to be satisfactory in order to observe several cycles of episodic convection). Solute concentration data was recorded to an output file every 60 days.

5.3. Numerical Modeling Results

[45] As a demonstrative and semiquantitative exercise in verifying the potential for episodic convection to occur, the numerical modeling was successful. Numerical experiments clearly confirm the existence of episodic convection and semiquantitatively validate the findings of the analytical approach. Figure 6 shows the evolution of the salt lake system through several convection "episodes." The model clearly showed a thickening of the saline boundary layer at the top due to evaporative concentration and diffusion, and once a critical threshold was reached (in terms of boundary layer thickness and density difference) convective fingering was clearly observed. As predicted by the analytical theory, the convection simultaneously dispersed solute throughout the model and eroded the boundary layer at the top, resulting in reduced instability and dissipation of the density driving force for convective fingering. After this dissipation period, evaporation leads to further evapoconcentration and diffusive boundary layer formation. As the boundary layer rethickens, a new convection episode begins as predicted by the newly proposed theory. Clearly the process will repeat for an extensive but finite period as the surface layer and subsurface groundwater concentration eventually become hypersaline and where salt precipitation occurs.

[46] Some other useful observations follow from the numerical modeling demonstration. In two dimensions, as in this model, it was clear that the onset and decay of convection is more complex than suggested by the 1-D theory. The onset and decay of fingering processes was shown to be temporally and spatially variable; while one finger was decaying in one region of the model, another could be growing and *vice versa*. The complete "birth" and "death" components of a convection episode was readily observable in localized regions or patches of the aquifer system, i.e., fingers grow and completely dissipate. On the larger layer scale, a more detailed analysis reveals that convection never completely dies throughout the entire layer. Rather than complete convective dissipation, there is substantial mixing away of the fingers and a large reduction in convection strength caused by dispersive mixing associated with the convective circulation. Episodicity is therefore observed through substantial changes in the strength of convection (strongest at the start of fingering process but weakening as dispersion mixes fingers away) rather than complete birth and death cycles. During these periods of lower strength convection, fingering never completely dies throughout the entire aquifer. Critically, however, completely new sets of fingers of progressively higher salinity continue to form with increasing time – an observation that is entirely consistent with the episodic convection hypothesis.

[47] On the basis of numerical simulations, a number of other semiquantitative observations can now be made.

These include: 1. The time between "convective births" increases nonlinearly with increasing number of convection cycles in the episodic convection process; 2. Once born, the "lifespan" of convective cycles increases nonlinearly with increasing time. Each progressive cycle is longer lived. For the hydrologic conditions employed in the demonstration numerical simulation, both successive birth and intermediate persistence timescales are approximately decadal to multidecadal – an observation consistent with the analytical theory; 3. Following the dissipation of the current convection episode, the time it takes for the next birth to occur is relatively constant among cycles and appears to be dictated by the diffusive timescales required to establish the necessary boundary layer thickness; 4. From animations of results not shown here, it is immediately evident that fingers at earlier time sink faster and mix away to death much more quickly. At later times, the newly introduced fingers grow more slowly and mix away to death more slowly. They have a longer life as noted above; and 5. Consequently, the system is significantly more dynamic at early stages in the system evolution and is obviously more lethargic at later times.

6. Discussion and Conclusion

[48] This study explored the transient evolution of a salt lake using an analysis based on the governing equations of flow and solute transport with a novel surface source term modeling the evaporative process. The transient dynamics of convective motion have been determined from an analytical and theoretical view point. For typical field-scale parameters, it has been shown that instability may initially occur within timescales on the order of weeks or decades and that a layer of salty fluid whose thickness is on the order of decimeters is responsible for the initial onset of convection. These spatial and temporal scales associated with convection have not been identified in previous literature and reveal significant new insights into the genesis of salt lake systems. Fascinatingly, the analysis has showed that when convection starts, the decimeter layer mixes and this results in the loss of the destabilizing force. In this period, the salty fluid diffuses downward. This results in a return to a hydrologic system where the salt profile is then well mixed throughout, but now with a background concentration with a higher average salinity. The process can then repeat for an extensive period. We have called this phenomenon episodic convection. Additionally, our analytical theory has shown that the critical Rayleigh number that should be employed in the case of an evaporating salt lake is somewhat lower than the traditional value of $4\pi^2$ first proposed by *Horton and Rogers* [1945] and then independently by *Lapwood* [1948]. Indeed, for the boundary conditions employed here (and critically in the presence of an upward discharge flux), we find that the appropriate choice of stability criterion yields $\mathrm{Ra}_{Dc} = 30$ approximately.

[49] Variable-density groundwater flow and solute transport modeling experiments of a field-based salt lake system confirm the existence of episodic convection and semiquantitatively validate the findings of the analytical approach. In local areas of the aquifer, complete birth and death processes are observed within an episodic convection cycle. Throughout the entire aquifer layer, episodicity is observed through substantial changes in the strength of convection (strongest at the start of fingering process but weakening as dispersion mixes fingers away) rather than complete birth and death cycles. Completely new sets of fingers of progressively higher salinity continue to form with increasing time – an observation that is entirely consistent with the episodic convection hypothesis. For the hydrologic conditions employed in the demonstration numerical simulation, both successive birth and intermediate persistence timescales are approximately decadal to multidecadal. As an approximate indication only, we may therefore expect that up to several hundred episodic convection cycles may occur throughout the evolution of a typical salt lake whose brine evolution timescales may be several thousand years. Clearly the number of cycles may be smaller or larger depending upon the brine evolution timescale as well as the episodicity timescales which are expected to be dependent on salt lake hydrogeologic parameters.

[50] Further work is required to assess the role of salt lake permeability and lake sediment strata in real geologic settings on this episodic convection process. *Simmons et al.* [2001] and *Nield and Simmons* [2007] have highlighted the critical role that heterogeneity in permeability may play in both the onset as well as growth and/or decay of free convective instabilities. Geologic heterogeneity may prove crucial in controlling the occurrence of the episodic convection problem and further work is required to assess this. The relationships between convective processes and heterogeneity are not simple [*Nield and Simmons*, 2007] and we therefore do not wish to extrapolate our findings here to heterogeneous geologic systems. Similarly, a fully 3-D assessment of mixed convection (including subhorizontal regional groundwater flow and discharge) in saline systems would be a useful area for future inquiry. Clearly discharge and evaporative processes (forced convection) occur simultaneously with the density-driven flow processes (free convection) and the relative strength of these processes is expected to control the spatial and temporal patterns of episodic convection. Finally, as noted by *Yechieli and Wood* [2002], different saline systems encountered in arid and semiarid regions throughout the world are similar in hydrologic terms but do vary in the nature of their boundary conditions. Therefore future analyses should explore the way in which hydrologic boundary conditions encountered in different saline system environments (salt pans, playas, sabkhas, salinas, saline lakes, and salt flats) effect both the likelihood and significance of the episodic convection process. It was considered beyond the scope of the current study to consider all possible saline systems. Similarly, future studies could examine the way in which chemical reactions and dissolution/precipitation processes influence episodic convection processes by way of chemically reactive transport modeling. The influence of double diffusive convection caused by simultaneous interaction of heat and solute transport may be another important consideration.

[51] To our knowledge, the proposed episodic convection process has not been identified or reported in previous salt lake literature. The analytical theory proposed is supported by a demonstration numerical example which clearly shows the nature of episodic convection in a simple aquifer setting. This study suggests that episodic convection processes may be important in understanding and interpreting data in salt lake hydrologic analyses and in explaining other observa-

tions relating to salt lakes - their salt accumulation, salt and water balances, isotope signatures, and other related hydrologic, hydrochemical, hydrogeologic, and climatological data that are related to salt lake studies. Field-based investigations will be critical to assess the existence of these phenomena in real geologic settings, but are likely to pose experimental challenges owing to the long timescales involved in these processes. Although theoretical, and perhaps somewhat preliminary, the results of this study suggest from a theoretical view point at least that this newly proposed episodic convection phenomenon clearly warrants further consideration in future salt lake hydrology research.

References

Caltagirone, J. P. (1982), Convection in a porous medium, in *Convective Transport and Instability Phenomena*, edited by J. Zierep and H. Oertel, pp. 199–232, G. Braun, Karlsruhe, Germany.

Diersch, H.-J. G. (2005), *FEFLOW: Finite Element Subsurface Flow and Transport Simulation System*, Inst. for Water Resour. Plann. and Syst. Res., Berlin.

Diersch, H.-J. G., and O. Kolditz (2002), Variable-density flow and transport in porous media: Approaches and challenges, *Adv. Water Resour.*, *25*, 899–944.

Duffy, C. J., and S. Al-Hassan (1988), Groundwater circulation in a closed desert basin: Topographic scaling and climate forcing, *Water Resour. Res.*, *24*, 1675–1688.

Fan, Y., C. J. Duffy, and D. S. Oliver (1997), Density-driven groundwater flow in closed desert basins: Field investigations and numerical experiments, *J. Hydrol.*, *196*, 139–184.

Holzbecher, E. (2005), Groundwater flow pattern in the vicinity of a salt lake, *Hydrobiologica*, *532*, 233–242.

Horton, C. W., and F. T. Rogers (1945), Convection currents in a porous medium, *J. Appl. Phys.*, *16*, 367–370.

Lapwood, E. R. (1948), Convection of a fluid in porous medium, *Proc. Camb. Philos. Soc.*, *44*, 508–521.

Macumber, P. G. (1991), *Interactions Between Groundwater and Surface Systems in Northern Victoria*, Victoria Dept. of Conserv. and Environ., Melbourne, Australia.

Nield, D. A. (1968), Onset of thermohaline convection in a porous medium, *Water Resour. Res.*, *11*, 553–560.

Nield, D. A. (1975), The onset of transient convective instability, *J. Fluid Mech.*, *71*, 441–454.

Nield, D. A., and A. Bejan (2006), *Convection in Porous Media*, 3rd ed., Springer, New York.

Nield, D. A., and C. T. Simmons (2007), A discussion on the effect of heterogeneity on the onset of convection in a porous medium, *Transp. Porous Media*, *68*, 413–421.

Rogers, D. B., and S. J. Dreiss (1995), Saline groundwater in Mono Basin, California: 2. Long-term control of lake salinity by groundwater, *Water Resour. Res.*, *31*, 3151–3169.

Rosen, M. R. (1994), The importance of groundwater in playas: A review of playa classifications and the sedimentology and hydrology of playas, *Spec. Pap. Geol. Soc. Am.*, *1468289*, 1–18.

Sanford, W. E., and W. W. Wood (2001), Hydrology of the coastal sabkhas of Abu Dhabi, United Arab Emirates, *Hydrogeol. J.*, *9*, 358–366.

Simmons, C. T., K. A. Narayan, and R. A. Wooding (1999), On a test case for density-dependent groundwater flow and solute transport models: The salt lake problem, *Water Resour. Res.*, *35*, 3607–3620.

Simmons, C. T., T. R. Fenstemaker, and J. M. Sharp Jr. (2001), Variable-density groundwater flow and solute transport in heterogeneous porous media: Approaches, resolutions and future challenges, *J. Contam. Hydrol.*, *52*, 245–275.

Simmons, C. T., K. A. Narayan, J. A. Woods, and A. L. Herczeg (2002), Groundwater flow and solute transport at the Mourquong saline-water disposal basin, Murray Basin, southeastern Australia, *Hydrogeol. J.*, *10*, 278–295.

Tyler, S. W., J. F. Muñoz, and W. W. Wood (2006), The response of playa and sabkha hydraulics and mineralogy to climate forcing, *Ground Water*, *44*, 329–338.

Weatherill, D., C. T. Simmons, C. I. Voss, and N. I. Robinson (2004), Testing density-dependent groundwater models: Two-dimensional steady state unstable convection in infinite, finite and inclined porous layers, *Adv. Water Resour.*, *27*, 547–562.

Wooding, R. A. (2007), Variable-density saturated flow with modified Darcy's law: The salt lake problem and circulation, *Water Resour. Res.*, *43*, W02429, doi:10.1029/2005WR004377.

Wooding, R. A., S. W. Tyler, and I. White (1997a), Convection in groundwater below an evaporating salt lake: 1. Onset of instability, *Water Resour. Res.*, *33*, 1199–1217.

Wooding, R. A., S. W. Tyler, P. A. Anderson, and I. White (1997b), Convection in groundwater below an evaporating salt lake: 1. Evolution of fingers or plumes, *Water Resour. Res.*, *33*, 1199–1217.

Yechieli, Y., and W. W. Wood (2002), Hydrogeologic processes in saline systems: Playas, sabkhas, and saline lakes, *Earth Sci. Rev.*, *58*, 343–365.

A. V. Kuznetsov, Department of Mechanical and Aerospace Engineering, North Carolina State University, Campus Box 7910, Raleigh, NC 27695-7910, USA.

D. A. Nield, Department of Engineering Science, University of Auckland, Private Bag 92019, Auckland 1142, New Zealand.

C. T. Simmons and J. D. Ward, School of Chemistry, Physics and Earth Sciences, Flinders University, GPO Box 2100, Adelaide, SA 5001, Australia. (craig.simmons@flinders.edu.au)